

Synthesis, Solvatochromic Analysis and Theoretical Studies of 3-((1H-benzo[d][1,2,3]triazole-1-yl)methyl)-4-phenylethyl-1H-1,2,4-triazole-5(4H)-thione

Zuhal KARAGÖZ GENÇ¹, Umut İbrahim OĞUZ², Murat GENÇ^{2*}

¹Adiyaman University Faculty of Pharmacy

²Adiyaman University Faculty of Arts and Sciences

(ORCID: 0000-0002-8847-9129) (ORCID: 0000-0003-1993-8819) (ORCID: 0000-0003-1224-4128)



Keywords: Benzotriazole, 1,2,4-triazole, DFT, Microwave irradiation, Docking

Abstract

The novel 2-(2-(1H-benzo[d][1,2,3]triazole-1-yl)acetyl)-N-phenylethyl hydrazinecarbothioamide (1) was synthesized by reaction of 2-(1H-benzo[d][1,2,3]triazole-1-yl)acetohydrazide and 2-phenylethylisothiocyanate. The condensation of compound 1 in presence of sodium hydroxide gave 3-((1H-benzo[d][1,2,3]triazole-1-yl)methyl)-4-phenylethyl-1H-1,2,4-triazole-5(4H)-thione (BPT). Theoretical calculations of BPT have been studied. The 6-311G+ (d,p) basis set was used for the DFT computations. The calculated spectra matched up with what was observed; hence the findings were confirmed. The same theoretical calculation procedure was used to examine BPT's LUMO, HOMO, and other associated energy values. To find out whether solute-solvent interactions were peculiar to BPT, the Catalán–Kamlet–Taft solvent parameter was used. Molecular docking studies were performed and identified the active sites of BPT with four anti-microbial receptors like *Aspergillus niger* (3EQA), *Hordeum vulgare* (1CNS), and *Candida Albicans* (4HOE) *Streptomyces* sp. (1CHK).

1. Introduction

In recent years, drug resistance has become a significant problem in the world, and in previous decades, multi-drug resistant gram-negative and gram-positive pathogenic bacteria caused lethal contagious diseases that affected the human population. Since the 1940s, penicillin has been used in human therapeutics; besides, various antibiotics have been used for 60 years. Firstly, antibiotics were not only developed to treat human infections but also used in veterinary, plant aquaculture, and agriculture [1, 2]. The extensive use of antibiotics caused a robust discerning burden that incommutably resulted in resistant bacteria spreading. The multifaceted mechanism for the advent of resistance has occurred: the resistance gene spread across the bacterial demesne with deceptive disregard for species barrier. However, the acquisition of resistance of genetic

factors has not been limited by the bacterial evolutionary response. Consequently, drug resistance has been developed as a global issue for human health that attracts the attention of scientists towards new antibacterial drug design and development. In this direction, heterocyclic compounds demonstrate their vital position because of varied biological activities [3, 4].

One of the heterocyclic compounds is 1,2,4-triazoles that contain three nitrogen atoms and two carbon atoms in a five-membered di-unsaturated ring structure [5].

Chemically speaking, 1,2,4-triazoles are a diverse group of molecules with numerous beneficial pharmacological properties. Some 1,2,4-triazole-based compounds have been shown to induce chemotherapeutic effects in cancer cells [6-10]. When it comes to drug design, N-heterocyclic molecules are critical [11-14]. triazoleMany classes of biologically

* Corresponding author: mgenç23@gmail.com

Received:08.04.2023, Accepted: 18.04.2023

active chemicals contain the molecule 1,2,4-triazole. 1,2,4-triazoles and their derivatives, in particular, are of great interest due to the vast range of biological activity they exhibit, such as anticancer [15], fungicidal [16-18], bactericidal [19-21], antioxidant [22], analgesic [23] and antidepressant [24] for these reasons, it was interesting to study 1,2,4-triazoles' vibrational spectra, electronic properties and molecular structure with the expectation that the results would be the helpful guide for future synthesis of more potent compounds and the prediction of their biological activity mechanism.

Due to our increased interest in search of new biological active agents having a 1,2,4-triazole ring, here we report an easy one-pot one component synthesis of the novel 1,2,4-triazole molecule, using NaOH, in good yield, and the present work also reports theoretical results of the synthesized compound to find structural characteristics by using DFT 6-311G+(d,p) methods..

2. Material and Method

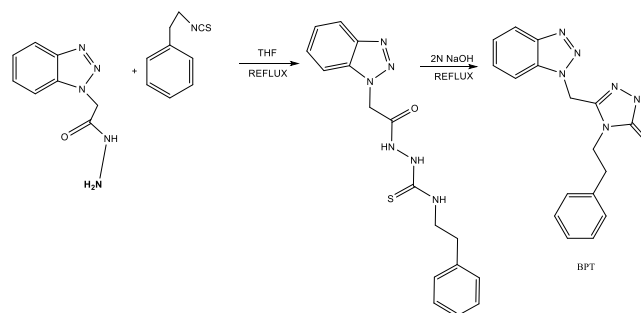
To produce compounds 1 and 2-(1H-benzo[d][1,2,3]triazole-1-yl)acetohydrazide (2), we followed the procedure outlined in the literature [25]. All chemicals were acquired from Merck and Sigma Aldrich and used without further purification.

2.1. Physical measurement

We used Perkin-Elmer FT-IR (ATR) to record the infrared spectra, a Stuart SMP 30 melting point apparatus to record the melting point, and an uncorrected analysis of both TMS (=0.0 ppm) was used as an internal standard to record ¹H and ¹³C-NMR spectra on the Bruker (300 MHz).

Synthesis of 3-((1H-triazolebenzotriazole-1-yl)methyl)-4-phenylethyl-1H-1,2,4-triazole-5(4H)-thione(BPT)

2-{2-(1H-benzotriazole-1-yl-acetyl)}-N-(3-phenylmethyl) hydrazincarbothioamid (CAS Registry Number 502869-56-9) (1g) was added to a 10 mL (2 N) solution of NaOH, and the combination was kept at reflux for 5 hours. After that, it was acidified with 37% conc. HCl and the pure product were produced by recrystallization in ethanol (Scheme 1).



Scheme.1. Synthetic pathway of 3-((1H-triazolebenzotriazole-1-yl)methyl)-4-phenylethyl-1H-1,2,4-triazole-5(4H)-thione(BPT)

M.p:188-190°C; FT-IR(ATR):3148(N-H), 3096-3037(CAr-H), 2851-2981(C-H), 1604(C=C), 758(C=S); ¹H-NMR(400MHz, DMSO-d₆) 12.50 (s, 1H, NH), 8.10 (s, 1H, Ar-H), 7.52 (s, 1H, Ar-H), 7.33(s, 1H, Ar-H), 7.40 (m, 4H, Ar-H), 7.24 (m, 2H, Ar-H), 5.12 (s, 2H, CH₂), 3.32 (t, 2H, CH₂, J=8Hz), 3.00 (t, 2H, CH₂, J=8Hz).. ¹³C-NMR(75MHz, DMSO-d₆): 168, 146, 137, 132, 129, 128, 127, 124, 120, 109, 46,41, 33. Anal. calcd for C₁₇H₁₆N₆S (336.41): C 60.69; H 4.79; N 24.98; S 9.53; found C 60.72; H 4.81; N 24.96; S 9.61. yield: 88%

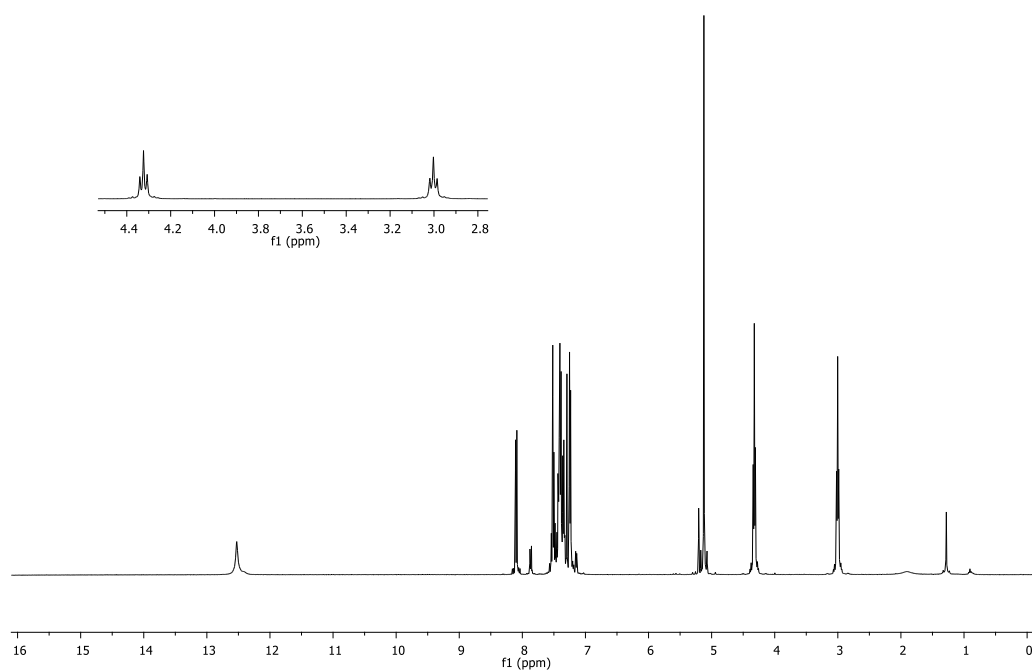


Figure 1. ¹H-NMR spectrum of (BPT)

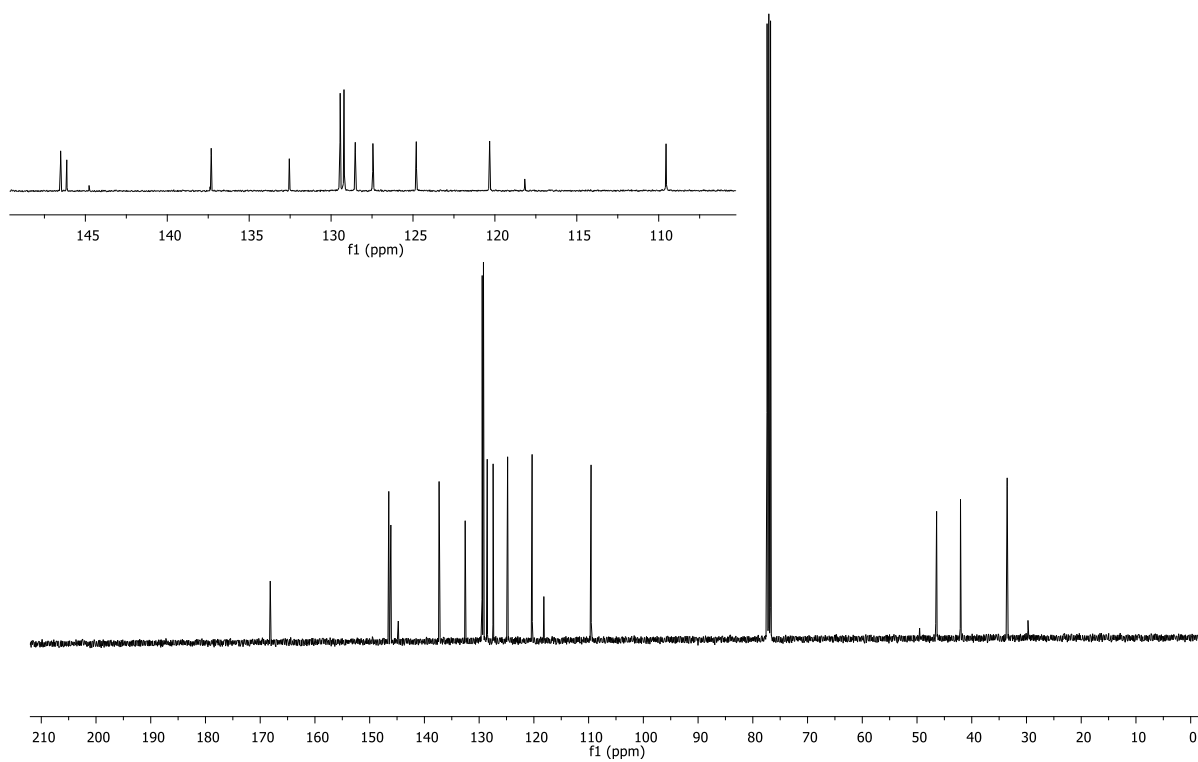


Figure 2. ¹³C-NMR spectrum of (BPT)

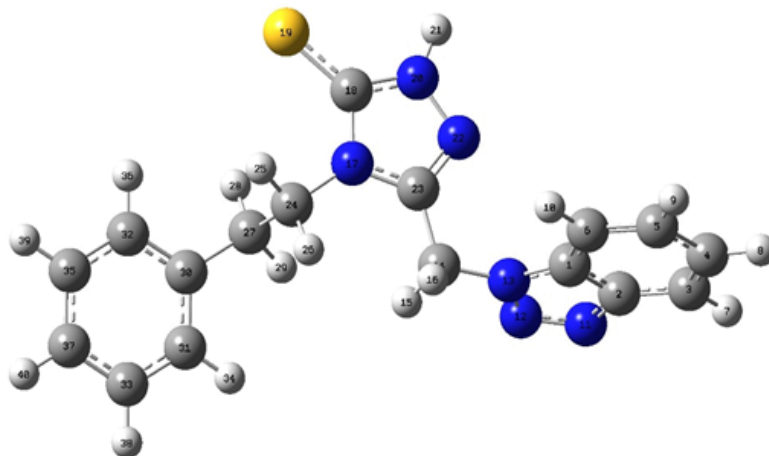


Figure 3. Optimized structure of BPT at B3LYP/6-311+(d,p) level

3. Theoretical study

The calculations for the molecular modelling were done with the Gaussian 09 software suite. Based on 6-311+G(d,p), the calculations were performed at the (DFT/B3LYP) technique. The molecule's vibrational frequencies were computed using the same quantum chemistry model's gas-phase equilibrium geometry. The Becke3-Lee-Yang-Parr (B3LYP) technique was used to include electron correlations [25]. Becke's gradient exchange corrections, Lee, Yang, and Parr correlation functional, and/or Vosko, Wilk, and Nusair correlation functional are all included in this [26].

3.1. Molecular geometry

The geometrical structure and atomic labelling of 3-((1H-benzo[d][1,2,3]triazole-1-yl)methyl)-4-phenylethyl-1H-1,2,4-triazole-5(4H)-thione have been computed and illustrated at Figure 3. the BPT's structural parameters have been optimized. Tables are given supplementary data. A partial double bond character has been discovered for all BPT ring bonds in the phenyl ring (S.Table 1) [27] that most of the phenyl ring's optimal bond lengths are similar in magnitude and lying between bond length ~ 1.40 Å to ~ 1.38 Å. Similarly, bond lengths of 1,2,4- triazole rings are between ~ 1.38 Å to ~ 1.29 Å.

Additionally, the smallest \angle (C24-N17-C14) and largest angle value (N17-C14-N13) of the molecule was computed at 98.50 and 140.

3.2. Atomic charge

Atomic charges perform a key role in a molecular system as electronic structure, molecular polarizability, dipole moment, atomic charge effect,

and the other molecular system properties. In addition, the asymmetric distribution of electrons in the chemical bond brings about certain charges. The calculated Mulliken atomic charges of BPT are shown in Fig.4.(S.Table 2) The charge distributions of molecules show the N atoms that bonded to a Substituent. The influence of the electron effect proceeds from hyperconjugation, and the inductive effect of Substituent groups in aromatic rings induces a particular negatively charged value in the aromatic carbon atoms. For the NBO, the natural atomic charges of BPT illustrate a similar tendency as Mulliken's atomic charges.

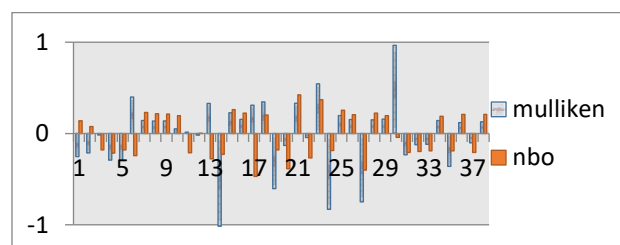


Figure 4. Graphical representations of atomic charges on the atoms of BPT

3.3. Frontier molecular orbital analysis

In terms of the BPT, the most critical molecular orbitals are HOMO-1, HOMO, LUMO, and LUMO+1. Using the B3LYP/6-311+ (d,p) technique, these orbital energies were figured out and delineated in Fig 5. The calculation showed that the charge distribution of the HOMOs level of BPT is highly delocalized on the 1,2,4-triazole (Fig 5). The charge density of the LUMO level is delocalized on the benzotriazole ring. It was concluded from the above

discussion that there is an electron flow from the 1,2,4-triazole to the Benzotriazole. The energy separation between the LUMO-HOMO orbital value is 4.32 eV.

Besides the absolute hardness (η), chemical potentials (μ), absolute electronegativities LUMO-HOMO energy gap (ΔE), global softness (S), global electrophilicity (ω), electronegativity (χ), absolute softness (σ), additional electronic charges (ΔN_{max}), have been calculated according to the following equations (S.Table 3) [28]

$$\eta = (|E_{LUMO} - E_{HOMO}|) / 2 \quad (1)$$

$$\chi = -(E_{LUMO} + E_{HOMO}) / 2 \quad (2)$$

$$\mu = -\chi \quad (3)$$

$$\sigma = 1 / \eta \quad (4)$$

$$\omega = (\mu)^2 / 2\eta \quad (5)$$

$$\Delta N_{max} = -(\mu) / 2\eta \quad (6)$$

$$S = 1 / 2\eta \quad (7)$$

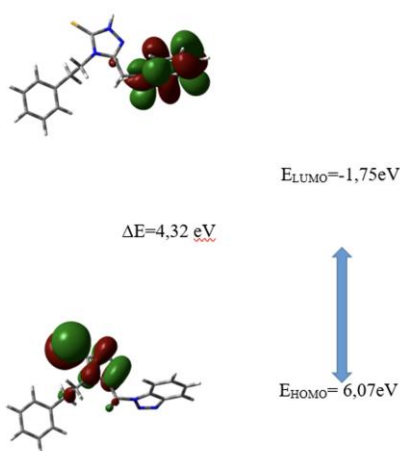


Figure 5. Calculated Frontier molecular orbitals of the title compound with DFT/B3LYP-G(d,p++)

3.4. NMR chemical shift analysis

The NMR spectroscopy is an essential technique for analyses of organic compounds. Geometry optimizations of BPT were performed with the DFT/B3LYP/semiempirical method/PM3 level basis set. After optimization, stage 1H and ^{13}C - NMR calculations of BPT were calculated GIAO [29-30] and 6-311+G (d,p) basis set in DMSO. Theoretical 1H and ^{13}C - NMR chemical shifts results of BPT

generally agree with the experimental chemical shift data.

The experimental and theoretical 1H and ^{13}C -NMR R2 values are 0,93 and 0,99, respectively and the atom positions, chemical shifts are generated in S.Table 4.

3.5. NBO Analysis

For investigating charge transfer or conjugative contact in molecular systems, NBO analysis guarantees an efficient method and ensures the research of intra- and intermolecular bonding and interaction in molecular systems [31]. There will be a more significant amount of giving tendencies from electron donors to electron acceptors, resulting in a longer E(2) value and, as a result, a more significant amount of conjugation throughout the entire system. There is a stable donor-acceptor interaction when electron density delocalization occurs between Lewis-type (bond or lone pair) Lewis NBO orbitals and formally empty non-Lewis NBO orbitals (anti-bond or Rydberg). NBO analysis used the second-order Fock matrix to look at intermolecular interactions. The stabilization energy associated with $I \rightarrow j$ delocalization is approximated as follows for each donor NBO (I) and acceptor NBO (j):

$$E(2) = \Delta E_{ij} = q_i = \frac{F(i,j)^2}{\epsilon_i \epsilon_j}$$

F_{ij} is the diagonal NBO fock matrix element of ϵ_i , ϵ_j , where q is the donor orbital occupied (orbital energies). DFT/B3LYP/6-311+(d,p) level NBO analyses have been undertaken, and the interaction LP (1) C2 \rightarrow π^* C1-N13 has the most excellent E(2) value around as shown in S.Table 5.

3.6. Molecular Electrostatic Potential (MEP) Analysis

To find out the net electrostatic effect caused by the entire charge distribution of the molecular and to correlate it with chemical reactivity, partial charges, dipole moments, and electro-negativity, we calculate the molecular electrostatic potential (MEP). It also makes it possible to understand the relative polarity using a visual approach [32,33]. The charge distribution of the molecule is shown in three dimensions in Figure 6 (below). There are three different electrostatic potential values in Fig 6: blue represents areas with the highest electrostatic potential, green indicates areas with zero potential, and red denotes areas with the lowest electrostatic

potential (see Fig 5). Red, orange, yellow, green, blue: these are the possible increments. The most vital repellent color is red, while the most robust attractive color is blue. An electronegative atom pair is frequently seen in regions of negative potential where there is a single atom. When looking at the MEP map of BPT, both the NH and the $-CH_2$ groups that joined the 1,2,4-triazole ring can be found in the positive zone. A look at Fig. 6 shows that a map of MEP values shows that negative potential exists over the benzotriazole group's N12 and N13 bonding atoms.

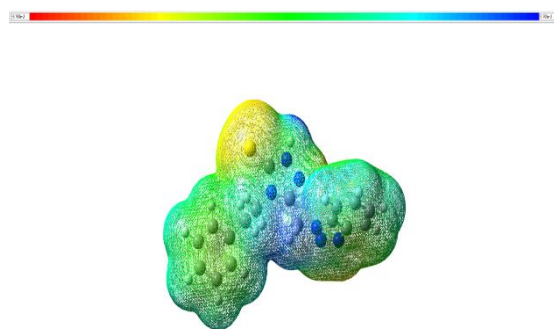


Figure 6. Molecular Electrostatic Potential (MEP) Analysis of BPT

3.7. Infrared Spectroscopy

In order to calculate the vibrational frequencies of BPT, the DFT/B3LYP method with the 6-311G+(d,p) basis set was utilized, as was the Gauss-View molecular visualization tool for the vibrational band assignments.

S.Table 6 shows theoretical computed IR spectra of the molecule's peaks. The measured and computed wave numbers agree very well. For two reasons, there could be a discrepancy between estimated and observed values. The first is that experimental data are in the solid phase, whereas theoretical calculations are in the gaseous phase. In addition, contrary to calculations, experimental values have been reported in the presence of intermolecular interactions.

The NH vibrations are the strong characteristic band for organic molecules [33,34]. NH stretching was observed at 3230 cm^{-1} in Raman and 3146 cm^{-1} in the IR spectrum while computed at 3668 cm^{-1} . Besides, NH in-plane bending vibration was observed at 1510, 1454 and 1205 cm^{-1} in Raman and 1495 and 1177 cm^{-1} in IR spectrum of the BPT while computed at 1496, 1550 and 1249 cm^{-1} . (Fig 7)

C-H stretching computed at 3203, 3185, 3173 cm^{-1} while was observed 3064, 3052 cm^{-1} in raman, 3093, 3037 cm^{-1} in IR spectrum. C-H bending was

observed 1485, 1324, 1152 cm^{-1} in IR, 1387, 1369, 1168 cm^{-1} in Raman spectrum.

C=N vibrations are also the other strong characteristic peaks of biomolecules. This peak vibration was observed 1625, 1591, 1590, IR, Raman, Theoretical spectrum, respectively.

In the case of N-N, vibrations were observed 1451, 1303 cm^{-1} in IR, 1454, 1348 in Raman spectrum while computed 1485, 1378 and 1359 cm^{-1} . (Fig 7)

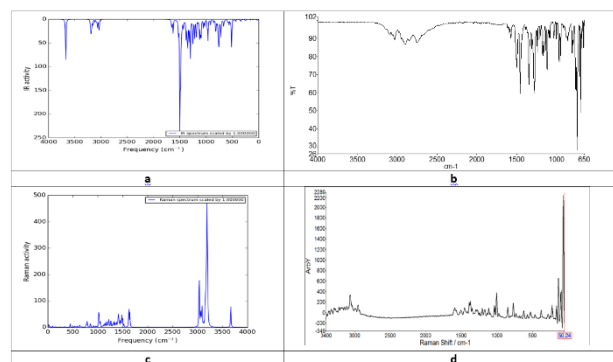


Figure 7. Experimental and theoretical vibration spectra of BPT (a= experimental FTIR spectrum, b= theoretical IR spectrum, c= experimental raman spectrum, d= theoretical raman spectrum)

3.8. Thermodynamic parameters

Rotation, vibration, and translation are all part of thermodynamics; hence they all matter. BPT's thermodynamic functional characteristics have been calculated using density functional theory (DFT). S.Table 7 contains estimated values that are useful for calculating biomolecular thermodynamic energy and predicting chemical reaction directions. To be clear, all of these thermodynamic calculations were done in the gas phase and could not be applied to the solution. Researchers looked examined BPT's thermodynamic characteristics between 100 and 1000 Kelvin. [36]. It was observed that enthalpy, entropy and heat capacity values increased depending on the temperature. The relevant equations are shown in Figure 8 and S.Table 7.

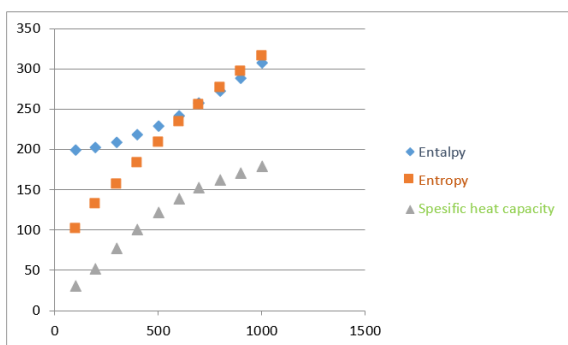


Figure 8. Thermodynamic Parameters of BPT

$$H^0_m = 73,40893 + 0,304215 T - 6,1 \cdot 10^{-5} T^2, \quad (R^2 = 0,9999)$$

$$S = 194,0431 + 0,029679T + 8,44 \times 10^{-5} T^2, \quad (R^2 = 0,9995)$$

$$CV = -085211 + 0,306056 T - 1,3 \times 10^{-4} T^2, \quad (R^2 = 0,9991)$$

3.9. Catalan and Kamlet-Taft solvatochromic parameters

UV spectra of BPT were taken in different solvents. The parameters affecting the absorbance bands of BPT were determined by the Catalan and Kamlet-Taft equations [36,37].

Catalan equation is given below.

$$V = aSA + bSB + cSp + dSdP$$

Catalan parameters are defined as solvent acidity (SA), solvent basicity (SB), solvent polarizability (SP) and solvent dipolarity (SdP).

Catalan equation was calculated as

$$V = 12.07 + 81.80SA + 12.44SB + 343.32SP + 25.38SdP$$

and $R^2 = 0.66$.

According to this equation, absorb and band is controlled SP ability.

The Kamlet-Taft equation is $V = V_0 + a\alpha + b\beta + c\pi^*$

The Kamlet-Taft solvent parameters are defined as the hydrogen bond donation ability (α), the hydrogen bond acceptor ability (β), the dipolarity-polarizability (π^*)

The Kamlet-Taft equation was calculated as $V = 231.60 + 50.62\alpha + 2.40\beta + 3.74\pi^*$ $R^2 = 0.24$. In regards to The Kamlet-Taft equation was found the most parameter as the hydrogen bond donation ability.

UV-Vis Spectrums of BPT were recorded with solvents of different polarities such as chloroform, THF, Ethanol, Pyridine, Formic acid. The experimental UV-Vis spectrum of BPT was observed a strong band of about 260 nm because of

$\pi \rightarrow \pi^*$ electronic transition. The computed wavelengths were recorded at about 315, 290, 281 nm, respectively. Hence, the electronic transition of $H \rightarrow L$ that is the most intense value was obtained at about 315 nm. The UV-Vis. parameters of BPT in different solvents are given in S. Table 8.

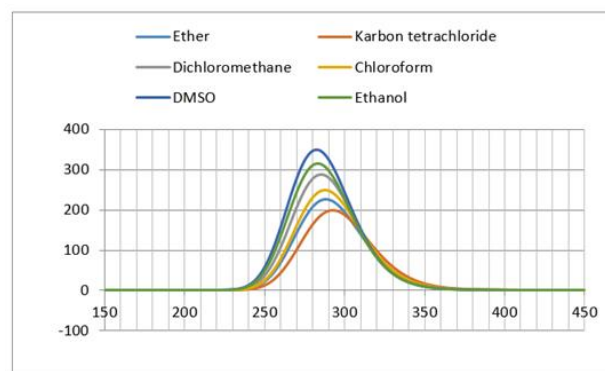


Figure 9. Theoretical UV Spectrum in Different solvents of BPT

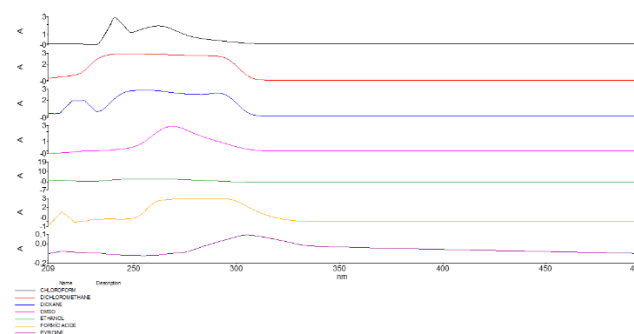


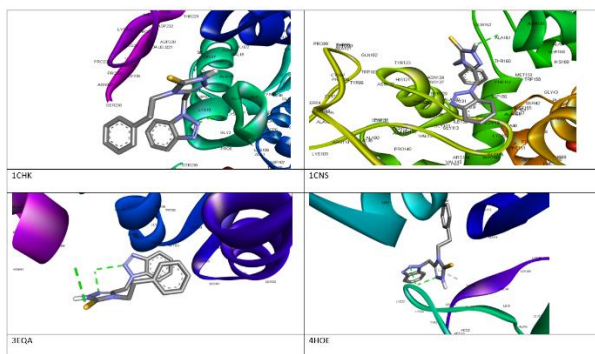
Figure 10. Experimental UV Spectrum in Different solvents of BPT

3.10. Molecular Docking

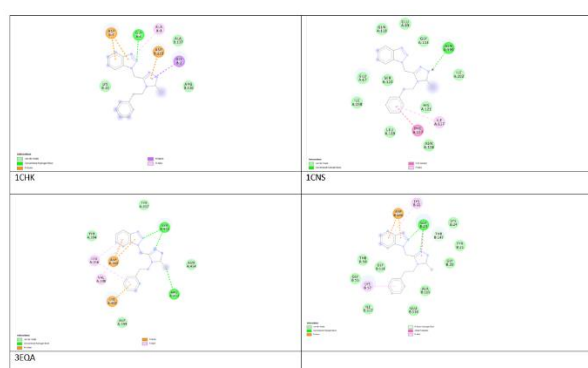
Molecular docking studies were performed by Autodock 4.2. We identified the active sites of BPT with four anti-microbial receptors like *Aspergillus niger* (3EQA), *Hordeum vulgare* (1CNS), and *Candida Albicans* (4HOE) *Streptomyces sp.* (1CHK) [38]. S. Table 9 summarizes the interactions and binding free energy in Kcal/mol between synthesized BPT and receptors. The binding energy of (1CHK), (1CNS), (3EQA) and (4HOE) are found to be 4.7, 7.3, 6.2 and 7.6 Kcal/mol, respectively.

Hybridizing benzotriazoles scaffold with 1,2,4-triazole ring moieties proved to be a favourable strategy in building up new molecules with good ability of the binding into the receptors binding site as triazole ring showed hydrogen bonding interactions

with ASN199 (1CHK), Er455, ARG453(3EQA), GLY23 (4HOE).



Figures 11. 3D Binding orientation of BPT with different proteins



Figures 12. 2D Binding orientation of BPT with different proteins.

4. Conclusion and Suggestions

Benzotriazole substitute 1,2,4-triazole was synthesized, FT-IR and NMR spectrums are studied both experimentally and theoretically. DFT (B3LYP) method using 6-311+G(d,p) basis set was used to compute the geometric parameters, vibrational frequencies, and chemical shifts of BPT's normal modes. Determine the charge transfer by performing a HOMO/LUMO study. The 1,2,4-triazole delocalizes the HOMO, while the benzotriazole delocalizes the LUMO. For ^1H and ^{13}C NMR, the chemical shifts agreed well with the DMSO solution's experimental results. By using NBO studies to explain molecular interaction and stability and the second-order perturbation for transactions, we have been able to stabilize the structure. Based on these

References

- [1] S. Rachakonda and L. Cartee, "Challenges in antimicrobial drug discovery and the potential of nucleoside antibiotics," *Curr. Med. Chem.*, vol. 11, no. 6, pp. 775–793, 2004

findings, we believe BPT is a viable candidate for further pharmacological and biochemical research. Clinical drugs containing triazole nucleus are being used in treating several ailments. The progress of resistance in *Candida* spp against fluconazole, the most effective anticandidal commercial drug, prompted the pharmacologist to synthesize triazole alcohols as fluconazole analogues to treat fluconazole-resistant fungal strains. 1,2,4-Triazole moiety via hydrogen bonding and dipole interaction can improve the solubility and affinity of the compounds with bimolecular targets. Among the broad spectrum of bioactivities, we comprehensively reviewed the advances in anticancer, anticonvulsant, antifungal, antibacterial, antiparasitic, analgesic antituberculosis anti-inflammatory and, antiviral, activities of 1,2,4-triazole derivatives particularly reported over the past decade. In according to the our study results; hybridizing benzotriazoles scaffold with 1,2,4-triazole ring moieties proved to be a favourable strategy in building up new molecules with good ability of the binding into the receptors binding site as triazole ring showed hydrogen bonding interactions.

Acknowledgment

If necessary, the people, institutions and organizations that helped in the study should be thanked for their help and support.

Contributions of the authors

(This part must be deleted in single-author articles)

The contributions of each author to the article should be indicated.

Conflict of Interest Statement

(This part must be deleted in single-author articles)

There is no conflict of interest between the authors.

Statement of Research and Publication Ethics

The study is complied with research and publication ethics

(Please write here ethics committee approval number and year, if any)

- [2] C. Nathan, "Antibiotics at the crossroads," *Nature*, vol. 431, no. 7011, pp. 899–902, 2004
- [3] K. Cheng, Q.-Z. Zheng, Y. Qian, L. Shi, J. Zhao, and H.-L. Zhu, "Synthesis, antibacterial activities and molecular docking studies of peptide and Schiff bases as targeted antibiotics," *Bioorg. Med. Chem.*, vol. 17, no. 23, pp. 7861–7871, 2009.
- [4] T. M. Barbosa and S. B. Levy, "The impact of antibiotic use on resistance development and persistence," *Drug Resist. Updat.*, vol. 3, no. 5, pp. 303–311, 2000.
- [5] K. S. Kiran, M. K. Kokila, Guruprasad, and Niranjana, "Crystal structure determination and molecular docking studies of 4-(5-Phenyl pyrazin-2-yl)-4h-1,2,4 Triazole-3-thiol with focal adhesion kinase inhibitors," *Open Chem. J.*, vol. 3, no. 1, pp. 69–74, 2016
- [6] Y. Sert, A. A. El-Emam, E. S. Al-Abdullah, A.-M. S. Al-Tamimi, C. Cırak, and F. Uçun, "Use of vibrational spectroscopy to study 4-benzyl-3-(thiophen-2-yl)-4,5-dihydro-1H-1,2,4-triazole-5-thione: A combined theoretical and experimental approach," *Spectrochim. Acta A Mol. Biomol. Spectrosc.*, vol. 126, pp. 280–290, 2014.
- [7] Y.-P. Hou et al., "Synthesis and antitumor activity of 1,2,4-triazoles having 1,4-benzodioxan fragment as a novel class of potent methionine aminopeptidase type II inhibitors," *Bioorg. Med. Chem.*, vol. 19, no. 20, pp. 5948–5954, 2011
- [8] A. Šermukšnytė, K. Kantminienė, I. Jonuškienė, I. Tumosienė, and V. Petrikaitė, "The effect of 1,2,4-triazole-3-thiol derivatives bearing hydrazone moiety on cancer cell migration and growth of melanoma, breast, and pancreatic cancer spheroids," *Pharmaceuticals (Basel)*, vol. 15, no. 8, p. 1026, 2022.
- [9] H. Alsaad, A. Kubba, L. H. Tahtamouni, and A. H. Hamzah, "Synthesis, docking study, and structure activity relationship of novel anti-tumor 1, 2, 4 triazole derivatives incorporating 2-(2, 3- dimethyl aminobenzoic acid) moiety," *Farmatsiia (Sofia)*, vol. 69, no. 2, pp. 415–428, 2022.
- [10] D. C. Kahraman, E. Bilget Guven, P. S. Aytac, G. Aykut, B. Tozkoparan, and R. Cetin Atalay, "A new triazolothiadiazine derivative inhibits stemness and induces cell death in HCC by oxidative stress dependent JNK pathway activation," *Sci. Rep.*, vol. 12, no. 1, p. 15139, 2022.
- [11] L. B. de O. Freitas et al., "Synthesis and antiproliferative activity of 8-hydroxyquinoline derivatives containing a 1,2,3-triazole moiety," *Eur. J. Med. Chem.*, vol. 84, pp. 595–604, 2014
- [12] V. Spanò et al., "Synthesis of a new class of pyrrolo[3,4-h]quinazolines with antimitotic activity," *Eur. J. Med. Chem.*, vol. 74, pp. 340–357, 2014.
- [13] R. Marulasiddaiah, R. G. Kalkhambkar, and M. V. Kulkarni, "Synthesis and biological evaluation of cyclic imides with coumarins and azacoumarins," *Open J. Med. Chem.*, vol. 02, no. 03, pp. 89–97, 2012.
- [14] P. Diana et al., "Synthesis and antitumor activity of 3-(2-phenyl-1,3-thiazol-4-yl)-1H-indoles and 3-(2-phenyl-1,3-thiazol-4-yl)-1H-7-azaindoles," *ChemMedChem*, vol. 6, no. 7, pp. 1300–1309, 2011.
- [15] Y.-P. Hou et al., "Synthesis and antitumor activity of 1,2,4-triazoles having 1,4-benzodioxan fragment as a novel class of potent methionine aminopeptidase type II inhibitors," *Bioorg. Med. Chem.*, vol. 19, no. 20, pp. 5948–5954, 2011.
- [16] A. C. Pasqualotto, K. O. Thiele, and L. Z. Goldani, "Novel triazole antifungal drugs: focus on isavuconazole, ravuconazole and albaconazole," *Curr. Opin. Investig. Drugs*, vol. 11, no. 2, pp. 165–174, 2010
- [17] J. Xu et al., "Design, synthesis and antifungal activities of novel 1,2,4-triazole derivatives," *Eur. J. Med. Chem.*, vol. 46, no. 7, pp. 3142–3148, 2011
- [18] C. Traträt et al., "Design, synthesis and biological evaluation of new substituted 5-benzylideno- 2-adamantylthiazol[3,2-b][1,2,4]triazol-6(5H)ones. Pharmacophore models for antifungal activity" *Arabian Journal of Chemistry*, vol.11, no. 4, pp. 573-590, 2018
- [19] G. V. Suresh Kumar, Y. Rajendraprasad, B. P. Mallikarjuna, S. M. Chandrashekar, and C. Kistayya, "Synthesis of some novel 2-substituted-5-[isopropylthiazole] clubbed 1,2,4-triazole and 1,3,4-oxadiazoles as potential antimicrobial and antitubercular agents," *Eur. J. Med. Chem.*, vol. 45, no. 5, pp. 2063–2074, 2010.
- [20] M. Strzelecka and P. Świątek, "1,2,4-triazoles as important antibacterial agents," *Pharmaceuticals (Basel)*, vol. 14, no. 3, p. 224, 2021.

- [21] A. A. El-Emam, A.-M. S. Al-Tamimi, M. A. Al-Omar, K. A. Alrashood, and E. E. Habib, "Synthesis and antimicrobial activity of novel 5-(1-adamantyl)-2-aminomethyl-4-substituted-1,2,4-triazoline-3-thiones," *Eur. J. Med. Chem.*, vol. 68, pp. 96–102, 2013.
- [22] A. Pachuta-Stec, "Antioxidant Activity of 1,2,4-Triazole and its Derivatives: A Mini-Review," *Mini Rev. Med. Chem.*, vol. 22, no. 7, pp. 1081–1094, 2022.
- [23] J. K. Sugden and T. O. Yoloje, "Medicinal applications of indole derivatives," *Pharm. Acta Helv.*, vol. 53, no. 3–4, pp. 65–92, 1978
- [24] "SciFinder® Login," Cas.org. [Online]. Available: <https://scifinder.cas.org/scifinder/view/scifinder/scifinderExplore.jsf>. [Accessed: 16-Jun-2023].
- [25] A. D. Becke, "Density-functional thermochemistry. III. The role of exact exchange," *J. Chem. Phys.*, vol. 98, no. 7, pp. 5648–5652, 1993
- [26] C. Lee, W. Yang, and R. G. Parr, "Development of the Colle-Salvetti correlation-energy formula into a functional of the electron density," *Phys. Rev. B Condens. Matter*, vol. 37, no. 2, pp. 785–789, 1988.
- [27] K. Wolinski, J. F. Hinton, and P. Pulay, "Efficient implementation of the gauge-independent atomic orbital method for NMR chemical shift calculations," *J. Am. Chem. Soc.*, vol. 112, no. 23, pp. 8251–8260, 1990.
- [28] K. Bahgat and S. Fraihat, "Normal coordinate analysis, molecular structure, vibrational, electronic spectra and NMR investigation of 4-Amino-3-phenyl-1H-1,2,4-triazole-5(4H)-thione by ab initio HF and DFT method," *Spectrochim. Acta A Mol. Biomol. Spectrosc.*, vol. 135, pp. 1145–1155, 2015
- [29] S. Muthu, T. Rajamani, M. Karabacak, and A. M. Asiri, "Vibrational and UV spectra, first order hyperpolarizability, NBO and HOMO-LUMO analysis of 4-chloro-N-(2-methyl-2,3-dihydroindol-1-yl)-3-sulfamoyl-benzamide," *Spectrochim. Acta A Mol. Biomol. Spectrosc.*, vol. 122, pp. 1–14, 2014
- [30] K. Bahgat and S. Fraihat, "Normal coordinate analysis, molecular structure, vibrational, electronic spectra and NMR investigation of 4-Amino-3-phenyl-1H-1,2,4-triazole-5(4H)-thione by ab initio HF and DFT method," *Spectrochim. Acta A Mol. Biomol. Spectrosc.*, vol. 135, pp. 1145–1155, 2015.
- [31] M. D. Diener and J. M. Alford, "Isolation and properties of small-bandgap fullerenes," *Nature*, vol. 393, no. 6686, pp. 668–671, 1998.
- [32] J.B. Foresman, E. Frisch Gaussian, Pittsburgh, PA, 1993. NIST Chemistry Webbook, IR database, <http://srdata.nist.gov/cccbdb>.
- [33] H.M. Jamroz, Vibrational energy distribution analysis: VEDA 4 program, Warsaw, 2004
- [34] A. Lakshmi and V. Balachandran, "Rotational isomers, NBO and spectral analyses of N-(2-hydroxyethyl) phthalimide based on quantum chemical calculations," *J. Mol. Struct.*, vol. 1033, pp. 40–50, 2013.
- [35] M. Genç, "Solvatochromic analysis and DFT computational study of N-(hexyl)-N-(5-(3-hydroxynaphthyl-2-yl)-1,3,4-oxadiazol-2-yl)amine," *Appl. Phys. A Mater. Sci. Process.*, vol. 125, no. 6, 2019.
- [36] J. Catalán and H. Hopf, "Empirical treatment of the inductive and dispersive components of Solute–Solvent interactions: The solvent polarizability (SP) scale: Inductive and dispersive components of Solute–Solvent interactions," *European J. Org. Chem.*, vol. 2004, no. 22, pp. 4694–4702, 2004
- [37] M. J. Kamlet, J. L. M. Abboud, M. H. Abraham, and R. W. Taft, "Linear solvation energy relationships. 23. A comprehensive collection of the solvatochromic parameters, .pi.*, .alpha., and .beta., and some methods for simplifying the generalized solvatochromic equation," *J. Org. Chem.*, vol. 48, no. 17, pp. 2877–2887, 1983.
- [38] S. M. Hiremath et al., "Synthesis of 5-(5-methyl-benzofuran-3-ylmethyl)-3H-[1, 3, 4] oxadiazole-2-thione and investigation of its spectroscopic, reactivity, optoelectronic and drug likeness properties by combined computational and experimental approach," *Spectrochim. Acta A Mol. Biomol. Spectrosc.*, vol. 205, pp. 95–110, 2018.